SUPPLEMENTAL MATERIAL

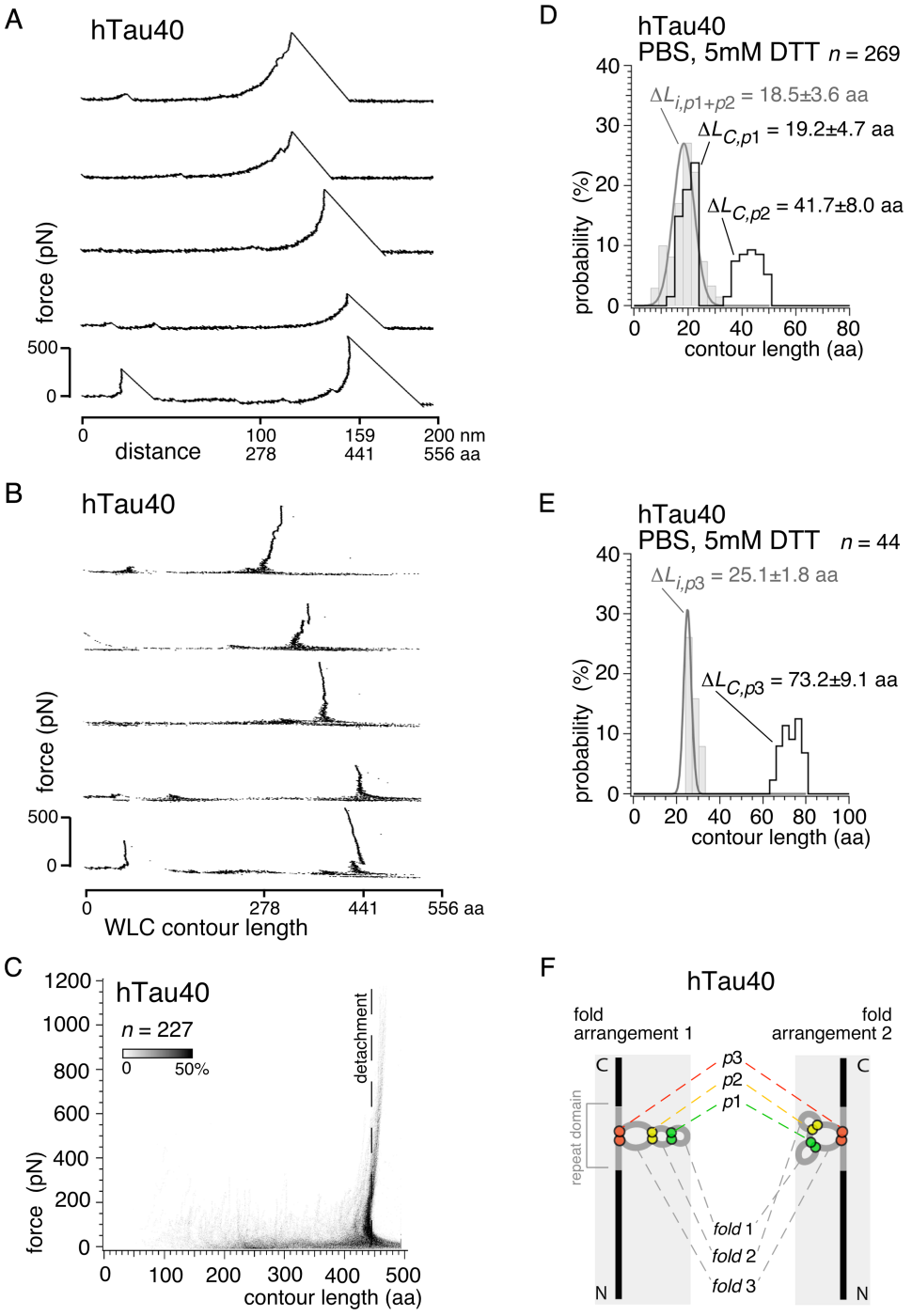

Supplemental Fig. S1. SMFS of hTau40. *A.* F-D curves recorded upon stretching single hTau40 molecules in PBS containing 5 mM DTT (same buffer as in Fig. 1*E*). *B.* Force-contour length (F-L_C) curves derived by transforming the F-D curves in (Fig. 1*E*) using the WLC model (see Materials&Methods). The position of the last force peak in each F-D (Fig. 1*E*) and F-L_C (*A*) curve reflects the detachment of the Tau molecule and assigns the contour length, L_C, in amino acids of the fully stretched molecule. Force peaks appearing at shorter L_C resemble interactions that unraveled upon

mechanically stretching of hTau40. *C.* Density plot of superimposed hTau40 F-L_C curves (n=227) that have been aligned on their detachment peaks. *D.* The length (most probable±SD) of the polypeptide segments, ΔL_i, that unraveled when rupturing the interactions at ΔL_C of 19.2±4.7 aa (p1) and 41.7±8.0 aa (p2) in hTau40 was determined from a Gaussian fit to the combined ΔL_i distribution of p1- and p2-interactions. *E.* The length of polypeptide segment, ΔL_i, embedded in the interaction at ΔL_C of 73.2±9.1 aa (p3) in hTau40 was determined from a Gaussian fit to the distribution as ~25 aa. *F.* Cartoon of hTau40 showing two likely arrangements of the folds in the hTau40 repeat domain (grey line) that is flanked by the unstructured termini (black lines). Interactions p1 (green circles), p2 (yellow), and p3 (red) that stabilize *fold*1, *fold*2, and *fold*3 are indicated. *n,* gives the number of analyzed F-D curves in *A*-*C* and of interactions in *D* and *E*.

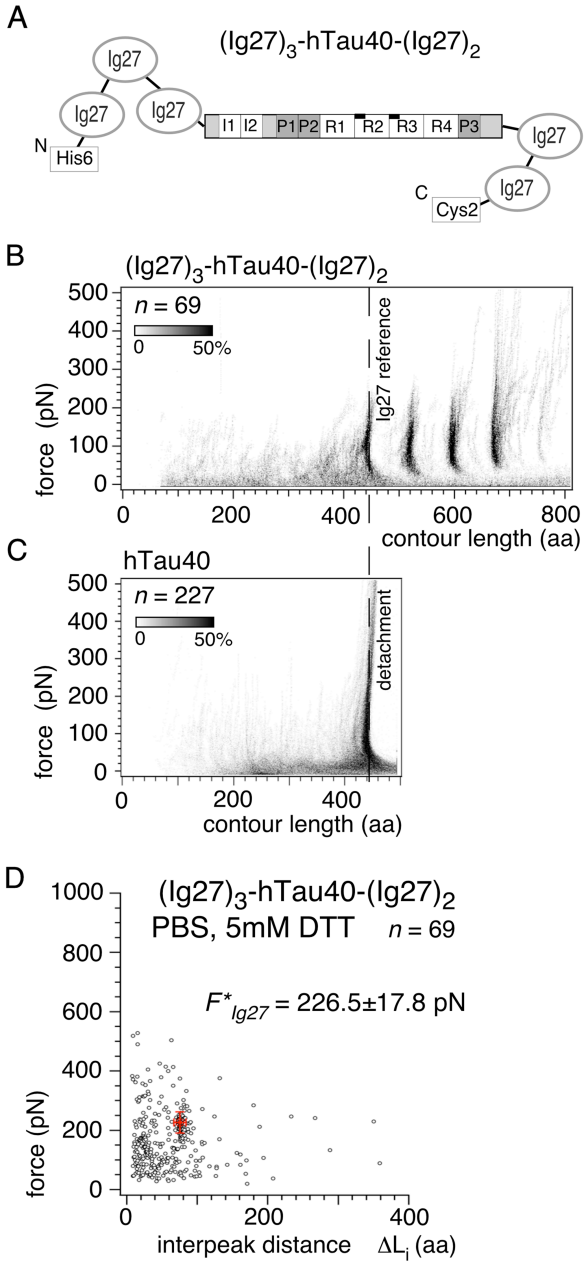

Supplemental Fig. S2. SMFS of the $(Ig27)_3$-hTau40-$(Ig27)_2$ construct. *A*. Fusion protein $(Ig27)_3$-hTau40-$(Ig27)_2$ flanking hTau40 by three N-terminal and two C-terminal immunoglobulin 27 (Ig27) domains. Full extension of hTau40 was guaranteed when detecting four or more Ig27 unfolding events in a F-D curve (see Fig. 3*B*). *B*. Density map of superimposed $(Ig27)_3$-hTau40-$(Ig27)_2$ F-L_C curves (n=69) that were aligned on the first force peak denoting the unfolding of Ig27. *C*. Density plot of superimposed hTau40 F-L_C curves (n=227) that have been aligned on their detachment peaks. *D*. Rupture forces of the $(Ig27)_3$-hTau40-$(Ig27)_2$ interactions analyzed in *E*. At a pulling velocity of 1000 nm/s, Ig27 has a characteristic rupture force of 226.5±17.8 pN (most probable±SD). The red data point indicates the average contour length of 77.5±4.7 aa and most probable force, F^* (±2SD), required to unfold Ig27. n, gives the number of analyzed F-D curves.

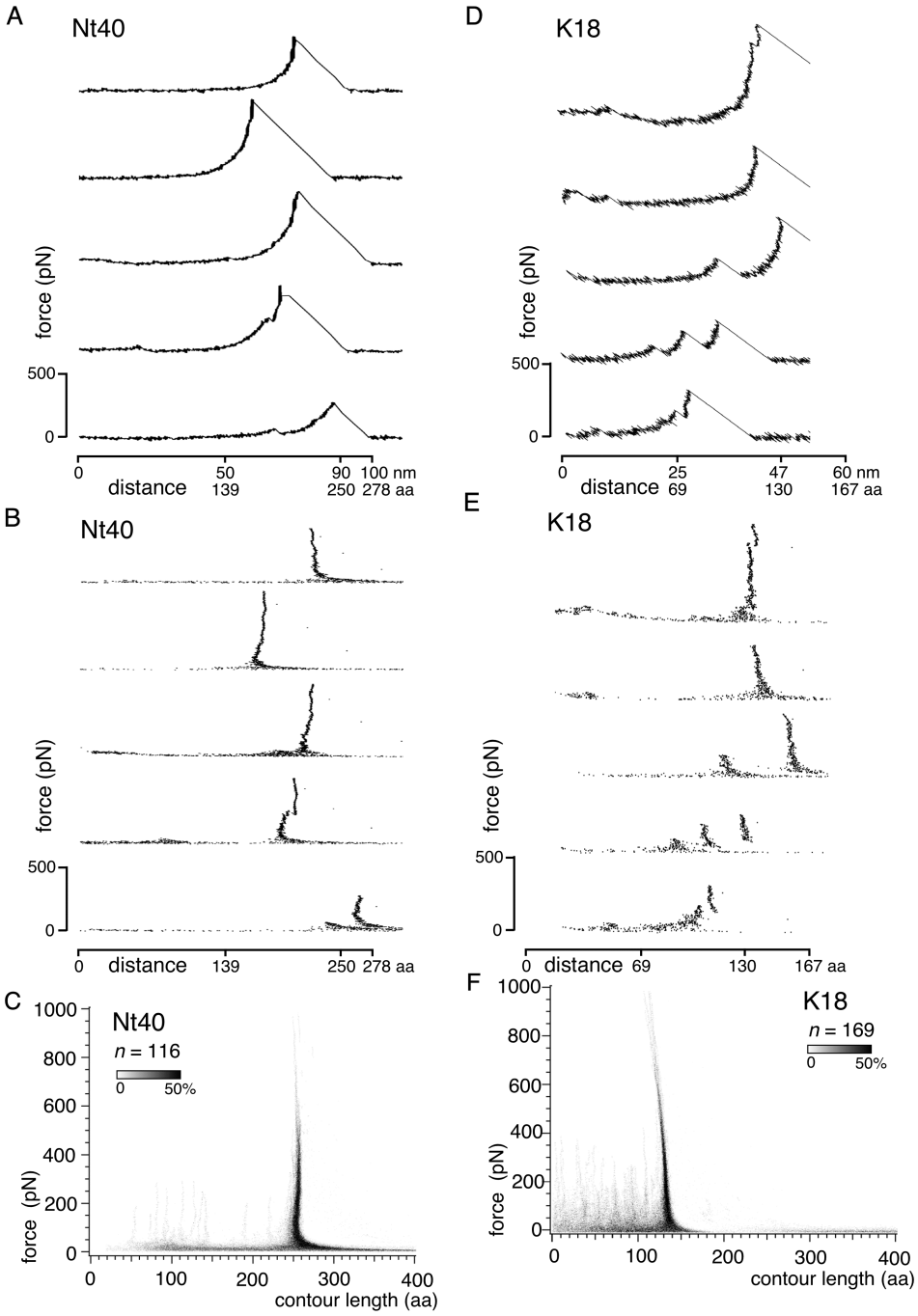

Supplemental Fig. S3. SMFS of Nt40, the 254 aa long N-terminal region of hTau40, and K18, the 4R-construct of hTau40. F-D curves recorded upon stretching single Nt40 (*A*) and K18 (*D*) molecules in PBS containing 5 mM DTT. F-L_C curves derived from F-D curves of Nt40 (*B*) and K18 (*E*) that are shown in (*A*) and (*D*). Density plots of superimposed Nt40 (*C*; *n*=116) and K18 (*F*; *n*=169) F-L_C curves that have been aligned on their detachment peaks. *n*, gives the number of analyzed F-D curves.

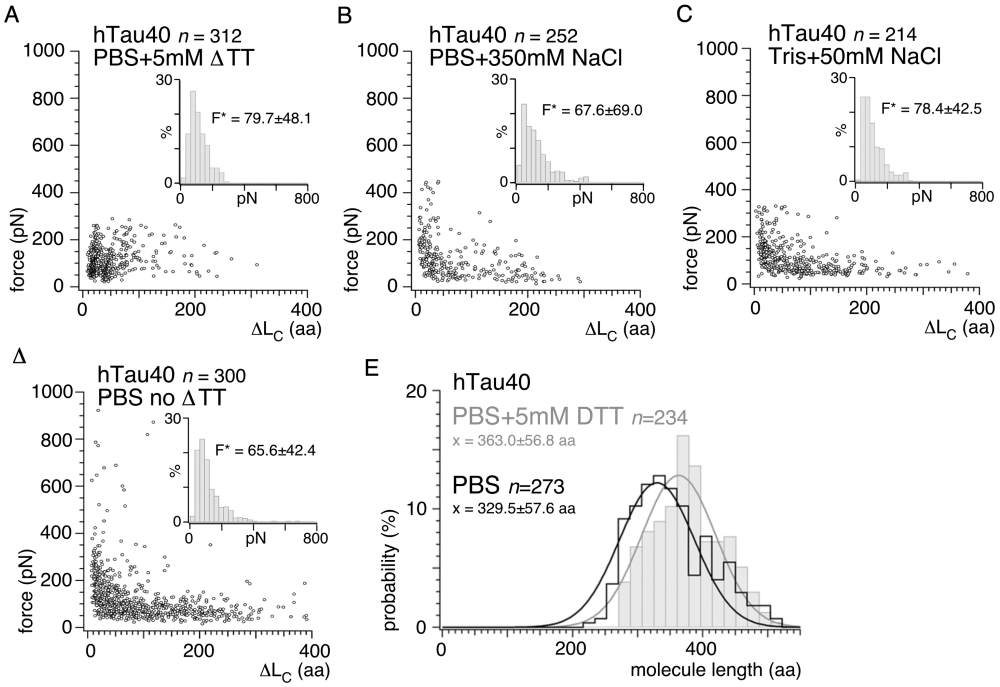

Supplemental Fig. S4. Interaction forces recorded upon mechanically stretching hTau40 in PBS, in high and in low ionic strength, and in absence of DTT. Rupture peak forces of hTau40 in (*A*) PBS containing 5 mM DTT (pulling velocity 875 nm/s), in (*B*) buffer of ~500 mM monovalent electrolyte (PBS + 5mM DTT + 350 mM NaCl; pulling velocity 1000 nm/s), in (*C*) buffer of ~50 mM monovalent electrolyte (10 mM Tris pH 7.4 + 5mM DTT + 50 mM NaCl; pulling velocity 1000 nm/s) and in (*D*) absence of DTT (pure PBS; pulling velocity 1000 nm/s). Insets show the force distribution and most probable forces (±SD). (*E*). Most probable contour lengths (aa) of stretched hTau40 molecules were determined from Gaussian fits to the distributions of detachment peak contour lengths detected for hTau40 in PBS containing 5mM DTT (grey) and in pure PBS (black). *n*, gives the number of analyzed F-D curves.

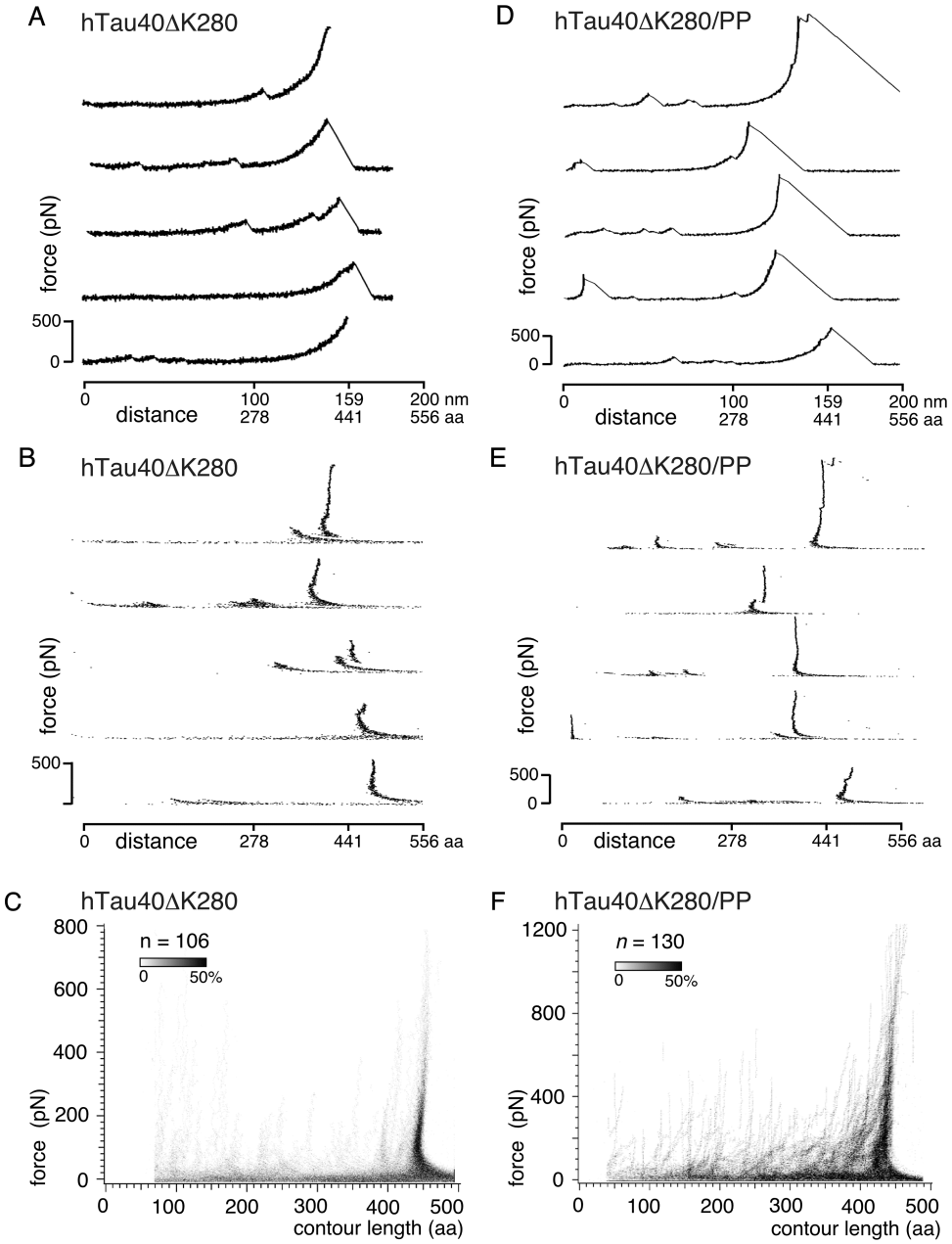

Supplemental Fig. S5. F-D curves recorded upon stretching hTau40ΔK280 (*A*) and hTau40ΔK280/PP (*D*) molecules in PBS containing 5 mM DTT. F-L_C curves derived from F-D curves of hTau40ΔK280 (*B*) and hTau40ΔK280/PP (*E*) shown in (*A*) and (*D*), respectively. Density plots of superimposed hTau40ΔK280 (*C*; *n*=106) and hTau40ΔK280/PP (*F*; *n*=130). F-L_C curves that have been aligned on their detachment peaks. *n*, gives the number of analyzed F-D curves.

Supplemental Table S1. Contour length distances to the detachment peak, ΔL_C (most probable±SD), and probabilities of rupture peaks detected in hTau40, K18, Nt40, hTau40ΔK280 and hTau40ΔK280/PP under the tested conditions (stretched in PBS + 5 mM DTT (*); pulling speed = 875 nm/s (^); pulling speed =1000 nm/s (^{V})). For hTau40ΔK280/PP, additional force peaks were detected at ΔL_C of 101.3±13.5 nm (*p*4) and 150.6±15.0 nm (*p*5). *n,* gives the number of analyzed F-D curves (molecules).

Interaction contour length distances (ΔL_C; most probable±SD) and probabilities in hTau40, hTau40ΔK280 and hTau40ΔK280/PP, and the constructs K18 and Nt40

	*p*1		*p*2		*p*3		ΔL_C>100 aa	total peaks/ molec	no peaks %	
	ΔL_C (aa)	%	ΔL_C (aa)	%	ΔL_C (aa)	%	peaks/molec			*n*
hTau40*^	19.2±4.7	52	41.7±8.0	34	73.2±9.1	14	0.15	1.67	32	312
K18*^{V}	19.2±4.7	21	41.7±8.0	29	73.2±9.1	10	0.01	1.23	21	375
Nt40*^{V}	19.2±4.7	8	41.7±8.0	7	73.2±9.1	8	0.13	0.63	50	452
hTau40*^{V} 500mM salt	19.2±4.7	17	41.7±8.0	16	73.2±9.1	7	0.33	1.16	12	250
hTau40*^{V} 50mM salt	19.2±4.7	31	41.7±8.0	26	73.2±9.1	21	0.57	2.10	16	204
hTau40*^{V} no DTT	19.2±4.7	29	41.7±8.0	32	73.2±9.1	22	0.96	2.54	11	300
hTau40 ΔK280*^	20.3±6.3	48	43.3±8.8	26	75.9±12.3	10	0.14	1.34	26	453
hTau40 ΔK280/PP*^{o}^	16.2±6.7	35	41.8±14.9	34	76.9±6.7	10	0.38	1.40	22	434
hTau40*^{V} heparin	19.2±4.7	22	41.7±8.0	29	73.2±9.1	24	1.30	2.94	14	477
hTau40 ΔK280*^{V} +heparin	20.3±6.3	21	43.3±8.8	25	75.9±12.3	27	1.87	3.14	7	244
hTau40 ΔK280/PP*^{V} +heparin	16.2±6.7	27	41.8±14.9	40	76.9±6.7	9	0.92	2.02	15	336

Supplemental Table S2. Most probable (±SD) interaction rupture forces and probabilities of force peaks detected at *p*1, *p*2, *p*3 and at ΔL_C >100 aa in hTau40, hTau40ΔK280 and hTau40ΔK280/PP under different buffer conditions (stretched in PBS + 5mM DTT (*); pulling speed = 875 nm/s (^); pulling speed =1000 nm/s (^{o})). In presence of 0.33 mM heparin, additional high-force interactions ($^\#$) were detected in hTau40 and hTau40ΔK280. *n,* gives the number of analyzed F-D curves. *ν*, gives the number of detected interactions.

Interaction rupture forces (most probable±SD) and probabilities in hTau40, hTau40ΔK280 and hTau40ΔK280/PP

	*p*1		*p*2		*p*3		DL_C>100 aa		
	force (pN)	*ν*	force (pN)	*ν*	force (pN)	*ν*	force (pN)	*ν*	*n*
hTau40*^	90.8±39.8	161	77.1±39.2	114	129.8±51.7	43	107.6±47.4	45	312
K18*^{o}	122.1±67.6	81	92.4±71.5	111	46.5±34.2	40	28.0±5.8	4	375
Nt40*^{o}	80.0±20.3	13	53.8±66.6	16	47.0±32.9	14	33.8±9.9	39	452
hTau40*^{o} 500mM salt	124.5±90.6	41	91.5±60.4	40	55.7±36.4	20	51.7±29.5	81	250
hTau40*^{o} 50mM salt	133.0±51.3	63	94.7±47.1	53	71.2±28.2	42	62.3±22.7	117	204
hTau40^o no DTT	155.6±84.7	86	92.8±47.6	95	76.3±28.6	65	66.4±29.1	287	300
hTau40 ΔK280*^	129.3±60.2	217	102.2±48.1	116	70.3±17.7	45	74.6±21.2	64	453
hTau40 ΔK280/PP*^	126.3±48.3	154	92.2±48.7	146	86.7±45.8	41	67.7±29.9	163	434
hTau40 +heparin*^{o}	165.0±112.9 545.1±96.1$^\#$	107	119.9±85.0 504.3±132.1$^\#$	137	93.3±58.4 232.7±31.6$^\#$	115	59.0±31.9 515.9±145.5$^\#$	621	477
hTau40 ΔK280 +heparin*^{o}	188.2±123.6 438.6±179.3$^\#$	52	86.3±58.7 643.7±223.5$^\#$	61	94.7±57.4 499.8±331.0$^\#$	68	70.0±40.8 448.6±214.9$^\#$	457	244
hTau40 ΔK280/PP +heparin*^{o}	145.0±62.1	92	91.4±59.1	135	69.5±47.1	30	45.5±23.4	311	336

Combination of force peaks in hTau40, hTau40ΔK280 and hTau40ΔK280/PP.

The separation between two rupture peaks depends on the length of polypeptide stretch that unfolds upon rupturing the first stabilizing interaction (1). So far we have assumed that the rupture peaks ΔL_C ~19 aa (*p*1), ~42 aa (*p*2), and ~73 aa (*p*3) resemble independent interactions of Tau. However, these interactions may also be linked to each other. To clarify this issue, we analyzed the combinations in which the peaks occurred (Supplemental Fig. S6).

The probability to detect a single force peak *p*1 (without a second in *p*2 or *p*3) was found in ~35% of hTau40, ~31% of hTau40ΔK280, and ~28% of hTau40ΔK280/PP. A combination of rupture peaks at *p*1 and *p*2 resembled the unfolding of two equally long ~19 aa polypeptide stretches. The probability of this case, P_{1+2}, is given by the product of the individual probabilities of *p*1 (P_1) and *p*2 (P_2), $P_{1+2}=P_2*P_1$. Experimentally, this probability was determined to be ~13%, ~11%, and ~4% for hTau40, hTau40ΔK280, and hTau40ΔK280/PP, respectively.

Assuming that the two force peaks *p*1 and *p*2 occur independent, representing two independent interactions *iA* and interactions *iB*, the overall probability for peak *p*1 would be given by a combination of the probabilities for *iA* (P_{iA}) and *iB* (P_{iB}) as $P_1 = (P_{iA}+P_{iB}) - (P_{iA}*P_{iB})$. The probability to have both independent peaks at *p*1 and *p*2 would be $P_{1+2} = (P_{i1}*P_{i2})$. This equation system could not be solved for the probabilities P_1 and P_{1+2} experimentally detected in hTau40 and hTau40ΔK280. From that it appeared that interaction *iB* depends on the presence of interaction *iA*, or *vice versa*.

Assuming that interaction *iB* depends on interaction *iA* ($P_{2B}=P_{1A+2B}/P_{1A}$), 37% of hTau40 molecules with interaction *iA* in *p*1 showed a second interaction *iB* at *p*2 (35% of hTau40ΔK280; 15% of hTau40ΔK280/PP). In case of hTau40ΔK280/PP (P_1=28% and P_{1+2}=4%), interactions *iA* and *iB* could be both independent and coupled.

A single force peak at position *p*2, reflecting a solitary interaction with a contour length of 42±6 aa, was detected in ~7% of hTau40 and hTau40ΔK280, and in ~4% of hTau40ΔK280/PP. Combinations of two interactions involving one ~19 aa and one ~42 aa interaction, namely [*p*2+*p*3] and [*p*1+*p*3], occurred in only ~2-4% of the F-D curves.

From this probability analysis it appears that the force peaks *p*1 and *p*2 resemble two ~19 aa interactions. In case of hTau40 and hTau40ΔK280, establishing the first interaction at *p*1 favors the second interaction at *p*2. The third interaction,*p*3 ,occurs independent of both *p*1 and *p*2. In hTau40ΔK280/PP, this folding hierarchy is disturbed and all three interactions appear independent of each other.

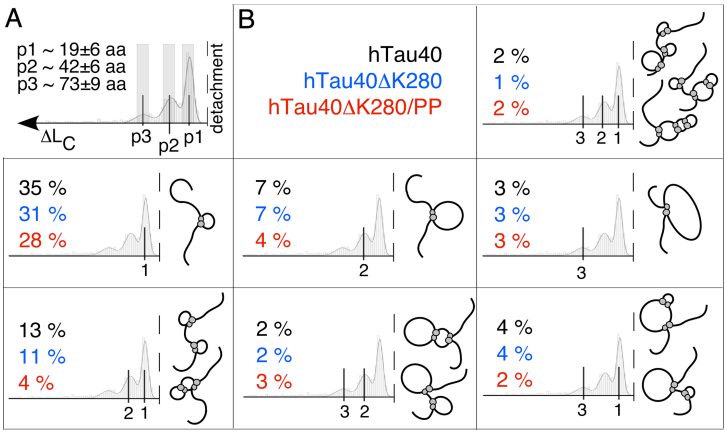

Supplemental Fig. S6. Combinations of interactions in hTau40, hTau40ΔK280 and hTau40ΔK280/PP. (*A*) Schematic assignment of the three frequent force peak positions *p*1, *p*2, and *p*3. (*B*) Probabilities (%) of detecting the indicated combination of force peaks *p*1, *p*2, and *p*3 for hTau40 (black), hTau40ΔK280 (blue), and hTau40ΔK280/PP (red). Probabilities and scenarios of other combinations of force peaks are shown.

Calculation of energy barrier heights and spring constants from DFS data.

Using DFS, the mechanical stability of molecular bonds is measured by the most probable rupture force, F^*, and the most probable loading rate, r^*_f. Both parameters can be used to describe the most prominent energy barrier that has to be overcome in direction of the reaction (pulling) coordinate, x (Supplemental Fig. S7A). The Bell-Evans theory (2, 3) describes the relation between F^*, r^*_f *and* x_u by

$$F^* = \frac{k_B T}{x_U} \ln\left(\frac{x_U r_f^*}{k_B T * k_0}\right) \qquad \text{(Eq. 1)}$$

where k_B is the Boltzmann constant and T the absolute temperature. x_u describes the distance from the free energy minimum in the bound state to the free energy maximum at the transition state (Supplemental Fig. S7A). k_0 is the transition (unfolding) rate of crossing the energy barrier at zero applied force. r^*_f was calculated for each peak in the F-D curves as $r^*_f = k_{mol} * \nu$, where k_{mol} is the spring constant of the molecule tethered between stylus and support and ν the pulling velocity. Rupture force and loading rate histograms were fitted to single Gaussian distributions. F^* was plotted semi-logarithmically against r^*_f. x_u and k_0 were estimated from non-linear least-square fits to Eq. 1. This was done for force peaks $p1$ (19±6 aa), $p2$ (42±6 aa), and $p3$ (73±9 aa) in the ΔL_C histograms for hTau40, hTau40ΔK280 and hTau40ΔK280/PP (Supplemental Fig. S7B-J).

The height of an energy barrier is given by the free energy difference, $\Delta G^{\ddagger}$, between bound and transition state (Supplemental Fig. S7A) of a bond. $\Delta G^{\ddagger}$ can be assessed using the Arrhenius equation

$$\Delta G^{\mp} = -k_B T \ln\left(\tau_D k_0\right) \qquad \text{(Eq. 2)}$$

where τ_D is the diffusive relaxation time ranging from 10^{-7} to 10^{-9} s for proteins (4). We used $\tau_D = 10^{-8}$ s as a fixed value throughout all calculations of the free energy barrier heights. In case of an error in τ_D, we would have generated a systematic error effecting $\Delta G^{\ddagger}$ of hTau40, hTau40ΔK280 and hTau40ΔK280/PP quantitatively but not relative to each other. The actual energy landscape shape of the force barriers is unknown. If assumed to resemble a simple parabolic energy potential, the spring constant of the bond, κ, can be derived from Eq. 3.

$$\kappa = \frac{2\Delta G^{\mp}}{x_u^2} \qquad \text{(Eq. 3)}$$

Errors in k_0, x_u and $\Delta G^{\ddagger}$ were propagated for estimation of errors in $\Delta G^{\ddagger}$ and κ.

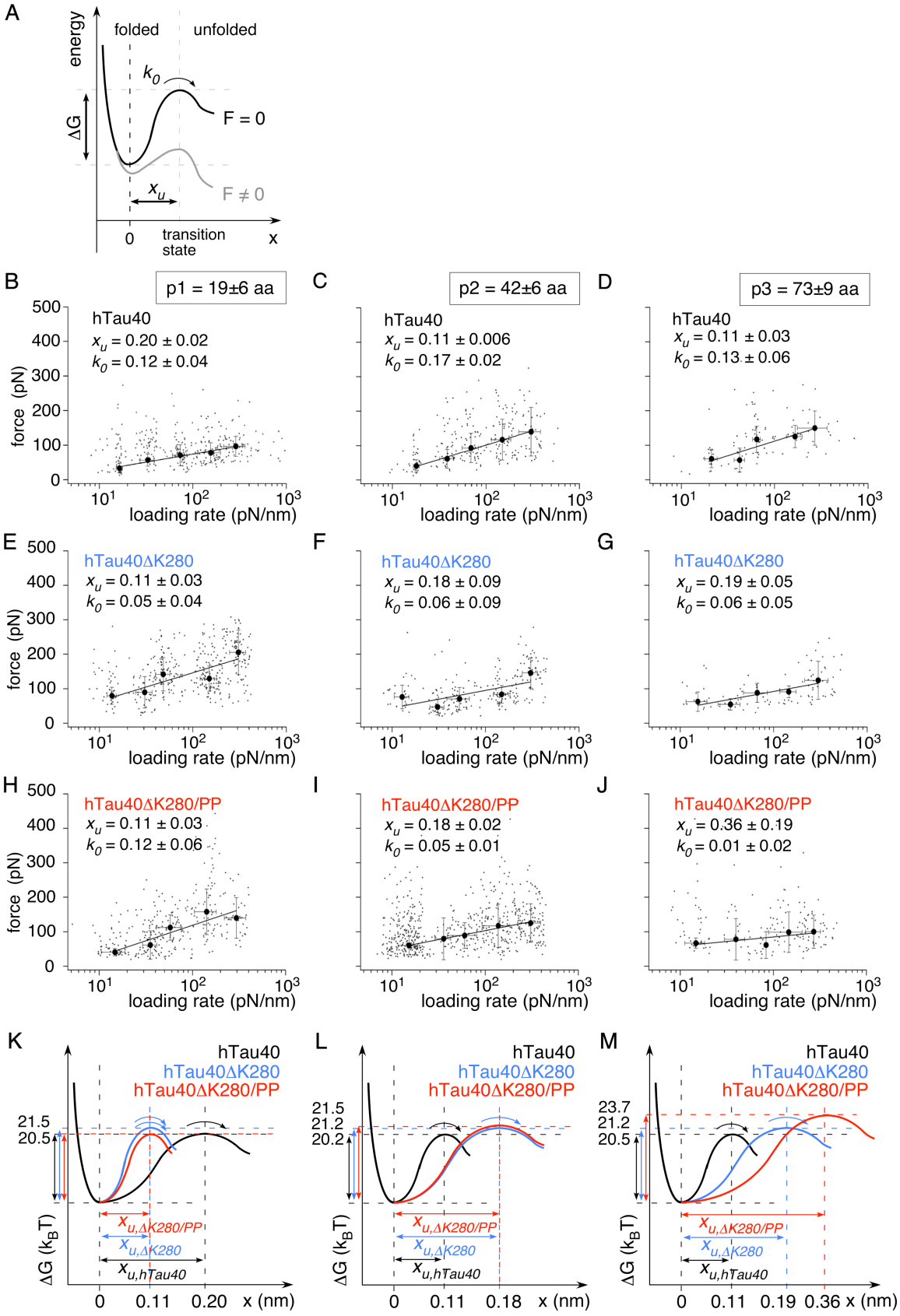
A
energy
folded
unfolded
k_0
ΔG
F = 0
F ≠ 0
x_u
0
transition state
x
B
p1 = 19±6 aa
hTau40
x_u = 0.20 ± 0.02
k_0 = 0.12 ± 0.04
C
p2 = 42±6 aa
hTau40
x_u = 0.11 ± 0.006
k_0 = 0.17 ± 0.02
D
p3 = 73±9 aa
hTau40
x_u = 0.11 ± 0.03
k_0 = 0.13 ± 0.06
E
hTau40ΔK280
x_u = 0.11 ± 0.03
k_0 = 0.05 ± 0.04
F
hTau40ΔK280
x_u = 0.18 ± 0.09
k_0 = 0.06 ± 0.09
G
hTau40ΔK280
x_u = 0.19 ± 0.05
k_0 = 0.06 ± 0.05
H
hTau40ΔK280/PP
x_u = 0.11 ± 0.03
k_0 = 0.12 ± 0.06
I
hTau40ΔK280/PP
x_u = 0.18 ± 0.02
k_0 = 0.05 ± 0.01
J
hTau40ΔK280/PP
x_u = 0.36 ± 0.19
k_0 = 0.01 ± 0.02
force (pN)
loading rate (pN/nm)
K
L
M
hTau40
hTau40ΔK280
hTau40ΔK280/PP
ΔG (k_BT)
$x_{u,ΔK280/PP}$
$x_{u,ΔK280}$
$x_{u,hTau40}$
x (nm)

Supplemental Fig. S7. DFS of frequent interactions in hTau40, hTau40ΔK280 and hTau40ΔK280/PP. *A*. Schematic free energy landscape for the forced unfolding of a folded structure. In absence of an externally applied force (F=0), an unfolding free energy barrier (black curve) is characterized by its height, $\Delta G^{\ddagger}$, the distance separating the folded from the transition state, x_u, and the unfolding rate in equilibrium, k_0. When applying an external force ($F\neq0$), the energy barrier tilts and lowers the free energy barrier (grey curve). As a result the height and the transition rate of the free energy barrier change. $\Delta G^{\ddagger}$, x_u, and k_0 can be estimated from dynamic SMFS performed at a broad range of pulling velocities (3). *B-J*. Dynamic force spectroscopy (DFS) spectra (F^* *vs.* $\log(l_r)$) of force peaks detected at ΔL_C of $p1$=19±6 aa (*B,E,H*), $p2$=42±6 aa (*C,F,I*), and $p3$=73±9 aa (*D,G,J*) for hTau40 and hTau40ΔK280 (pulling velocities: 104, 249, 497, 1249, 2490 nm/s) and hTau40ΔK280/PP (pulling velocities: 104, 256, 497, 1090, and 2490 nm/s). The raw data is plotted as scatter plot in the background of the DFS spectra. (*K-M*) Schematic unfolding energy barriers determined from the DFS spectra (*B-J*) for the interactions at $p1$ (*K*), $p2$ (*L*), and $p3$ (*M*) in hTau40 (black), hTau40ΔK280 (blue), and hTau40ΔK280/PP (red).

Supplemental Table S3. Parameters characterizing the unfolding energy barriers (Supplemental Fig. S7A) of force peaks at $p1$=19±6 aa, $p2$=42±6 aa, and $p3$=73±9 aa in hTau40, hTau40ΔK280 and hTau40ΔK280/PP stretched in PBS + 5mM DTT (pulling velocities 104, 249, 497, 1249 and 2490 nm/s (^); pulling velocities 104, 256, 497, 1090 and 2490 nm/s (^{o})). The distance from the folded to the transisition state, x_u, and the native transition rate, k_0, were derived from fitting (Supplemental material Eq. 1) the DFS spectra (Supplemental. S7B-J). The free energy difference, $\Delta G^{\ddagger}$ (Supplemental material Eq. 2), and the interaction spring constant, κ (Supplemental material Eq. 3), of energy barriers were calculated from x_u and k_0.

DFS fit values and energy barrier characteristics for interactions in hTau40, hTau40ΔK280 and hTau40ΔK280/PP

	$p1$		$p2$		$p3$	
	x_u (nm)	k_0 (s^{-1})	x_u (nm)	k_0 (s^{-1})	x_u (nm)	k_0 (s^{-1})
hTau40^	0.20±0.02	0.12±0.04	0.11±0.01	0.17±0.02	0.11±0.04	0.13±0.06
hTau40 ΔK280^	0.11±0.03	0.05±0.04	0.18±0.09	0.06±0.09	0.19±0.05	0.06±0.05
hTau40 ΔK280/PP^o	0.11±0.03	0.12±0.06	0.18±0.02	0.05±0.01	0.36±0.19	0.01±0.02
	κ (N/m)	$\Delta G^{\ddagger}$ (k_BT)	κ (N/m)	$\Delta G^{\ddagger}$ (k_BT)	κ (N/m)	$\Delta G^{\ddagger}$ (k_BT)
hTau40^	4.2±0.8	20.5±0.3	13.7±2.5	20.2±0.1	13.9±10.1	20.5±0.5
hTau40 ΔK280^	14.5±7.9	21.4±0.8	5.4±5.4	21.2±1.5	4.8±2.6	21.2±0.8
hTau40 ΔK280/PP^o	13.9±7.6	20.5±0.5	5.4±1.2	21.4±0.2	1.5±1.5	23.0±2.0

REFERENCES

1. Rief, M., Gautel, M., Oesterhelt, F., Fernandez, J. M. and Gaub, H. E. (1997) *Science* **276**, 1109-1112
2. Bell, G. I. (1978) *Science* **200**, 618-627
3. Evans, E. and Ritchie, K. (1997) *Biophys J* **72**, 1541-1555
4. Krieger, F., Fierz, B., Bieri, O., Drewello, M. and Kiefhaber, T. (2003) *J Mol Biol* **332**, 265-274